Proc. Natl. Acad. Sci. USA
Vol. 76, No. 1, pp. 33–37, January 1979
Chemistry

Resonance Raman studies of bathorhodopsin: Evidence for a protonated Schiff base linkage

(retinal conformations/visual excitation/kinetics/multichannel detection)

GREGORY EYRING AND RICHARD MATHIES

Chemistry Department, University of California, Berkeley, California 94720

Communicated by Melvin Calvin, November 8, 1978

ABSTRACT **A dual beam pump/probe laser technique has been used with a 585-nm probe wavelength to obtain maximal resonance enhancement of the Raman lines of bathorhodopsin in a photostationary steady-state mixture at −160°C. These studies show that bathorhodopsin has a protonated Schiff base vibration at 1657 cm^{-1} which shifts upon deuteration to 1625 cm^{-1}. Within our experimental error (±2 cm^{-1}) these frequencies are identical to those observed in rhodopsin and isorhodopsin. These effects show that the strength of the C=N bond and the degree of protonation of the Schiff base nitrogen are the same in bathorhodopsin, rhodopsin, and isorhodopsin. The implications of these results for the structure of the retinal chromophore in bathorhodopsin are discussed. The resonance Raman spectrum of pure bathorhodopsin has been generated by accurately subtracting the residual contributions of rhodopsin and isorhodopsin from spectra of the low temperature photostationary mixture. Bathorhodopsin is found to have lines at 853, 875, 920, 1006, 1166, 1210, 1278, 1323, 1536, and 1657 cm^{-1}. Also, by using an intensified vidicon detector, we have observed Raman scattering from bathorhodopsin at room temperature by generating a photostationary steady state with pulsed laser excitation. At room temperature the three characteristic lines of bathorhodopsin are found at 858, 873, and 920 cm^{-1}. The fact that the frequencies of these bathorhodopsin lines are nearly identical at both temperatures implies that the retinal conformation in bathorhodopsin formed at −160°C is the same as that formed at room temperature.**

Early studies (1–3) on the mechanism of visual excitation demonstrated that rhodopsin, the visual pigment in vertebrate rod cells, contains an 11-*cis* retinal chromophore that is isomerized to an all-*trans* conformation after photon absorption. This led logically to the conclusion that the primary photochemical event was a *cis* → *trans* photoisomerization about the 11,12 double bond. However, recent work has begun to question this simple model. Picosecond absorption measurements (4) demonstrated that the first photolytic intermediate, bathorhodopsin, is formed in less than 6 psec at room temperature. It was felt that this time was too short to permit the complete isomerization of the chromophore. Also, resonance Raman measurements by Oseroff and Callender (5) showed that bathorhodopsin has intense Raman lines at frequencies (856, 877, and 920 cm^{-1}) that are not found in the Raman spectrum of the all-*trans* protonated Schiff base derivative of retinal. They therefore concluded that the formation of bathorhodopsin might not involve a simple *cis* → *trans* isomerization about the 11-*cis* double bond. Subsequently, it has been proposed (6–8) that the initial photochemical event that leads to the formation of bathorhodopsin is a proton translocation. This hypothesis has been supported by recent picosecond absorption measurements (8) on the rate of formation of bathorhodopsin. This proton translocation might proceed to form a carbonium ion, exomethylene, or retroretinal structure, as depicted in Fig. 1. A common feature of these models is that the formation of bathorhodopsin is associated with the reduction of the bond order of the C=N double bond at the C-15 position and the increase of the H—N bond order on the Schiff base nitrogen. It must be noted, however, that the proton translocation hypothesis has been questioned by several authors (9–11) on the basis of the interconvertibility of rhodopsin, bathorhodopsin, and isorhodopsin (see Fig. 2). More detailed information about the conformation of bathorhodopsin is needed in order to resolve this controversy.

We have chosen resonance Raman spectroscopy to investigate the visual pigment system for two reasons. First, Raman spectra of these pigments show great sensitivity to the conformational structure of the retinal chromophore (12). Second, selective resonance enhancement permits the assignment of particular Raman lines to specific molecules in the photostationary steady state (5). These experiments have already been used to examine the conformation and interactions of the retinal chromophore in rhodopsin, isorhodopsin, and several of their photolytic intermediates (5, 12–16). One objective of this study was to obtain a spectrum of bathorhodopsin that would provide information on the strength of the C=N bond at the C-15 position and on the degree of protonation of the Schiff base nitrogen. In addition, we wanted to compare the scattering of bathorhodopsin in the conformationally sensitive fingerprint region (1100–1400 cm^{-1}) with that of model retinal compounds.

The principal technique we used was developed by Oseroff and Callender (5). They took advantage of the fact that below −140°C irradiation of rhodopsin produces a photostationary steady-state mixture containing only rhodopsin, isorhodopsin, and bathorhodopsin (3) (Fig. 2). As shown by Yoshizawa and Wald (3), the relative proportions are strongly dependent on the irradiation wavelength. Qualitatively, irradiation with blue light (488 nm), which both rhodopsin and isorhodopsin absorb strongly, will produce a large population of bathorhodopsin, whereas irradiation with yellow light (585 nm), which bathorhodopsin absorbs but the others do not, will deplete the amount of bathorhodopsin in the steady state. If a sample of rhodopsin is irradiated at 77 K with a laser beam near the absorption maximum of bathorhodopsin (543 nm), the Raman scattering from bathorhodopsin is resonantly enhanced more than that from rhodopsin and isorhodopsin. However, as discussed above, the percentage of bathorhodopsin in the photostationary steady state is small. The amount of bathorhodopsin can be increased by adding a second coaxial pump laser beam that is maximally absorbed by rhodopsin and isorhodopsin. The resulting Raman spectrum is dominated by bathorhodopsin, and it is possible to subtract the contributions of rhodopsin and isorhodopsin to produce a "pure" bathorhodopsin spectrum.

Another pertinent question is whether the characteristic lines of bathorhodopsin at 856, 877, and 920 cm^{-1} (5) can be observed at room temperature. The fact that these unique vi-

The publication costs of this article were defrayed in part by page charge payment. This article must therefore be hereby marked "*advertisement*" in accordance with 18 U. S. C. §1734 solely to indicate this fact.

Abbreviations: OMA, optical multichannel analyzer; CW, continuous wave.

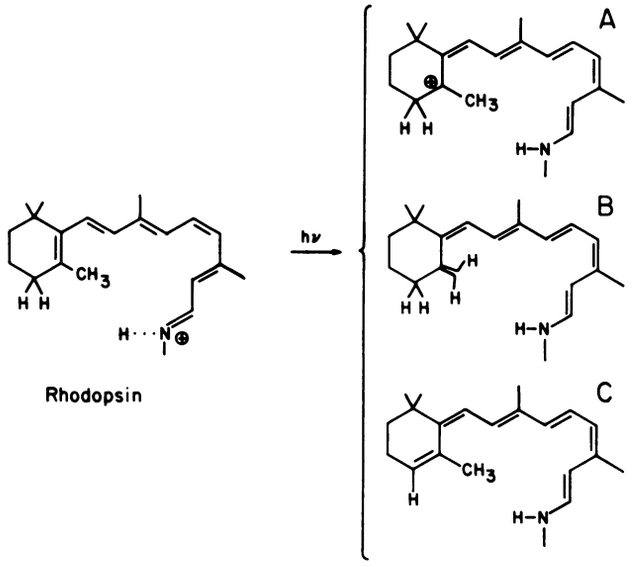

FIG. 1. Proposed proton translocation models for bathorhodopsin. In model A (carbonium ion), a single proton is transferred to the Schiff base nitrogen. Models B (exomethylene) and C (retroretinal) involve, in addition, the simultaneous removal of a proton from the β-ionone ring system.

brations are not seen in the all-*trans* model compounds suggests that the chromophore of bathorhodopsin has not attained a relaxed all-*trans* conformation. One possible explanation is that the frozen protein matrix artificially constrains the chromophore. This can be tested by generating a Raman spectrum of bathorhodopsin at room temperature with high-intensity laser pulses.

MATERIALS AND METHODS

Frozen bovine retinas were purchased from Hormel and rod outer segments were isolated by a sucrose flotation method (17). Ammonyx LO (Onyx Chemical Co., Jersey City, NJ) solubilized rhodopsin was purified by hydroxylapatite chromatography (18), concentrated by vacuum dialysis (Schleicher and Schuell), and diluted 2:1 with glycerol. We prepared deuterated samples by exchanging the concentrate with ^2H_2O and diluting 2:1 with deuterium-exchanged glycerol. The final Raman samples had an absorbance of 2.0 (1 cm) at 500 nm.

The rhodopsin was placed in a glass capillary and mounted beside an iron/constantan thermocouple in a glass dewar. Cold nitrogen was blown over the capillary until the temperature reached −160°C. We obtained Raman spectra of purified pigments without glycerol in the same dewar by rapidly freezing Ammonyx LO-solubilized rhodopsin (0.4 mM) in direct contact with a copper block.

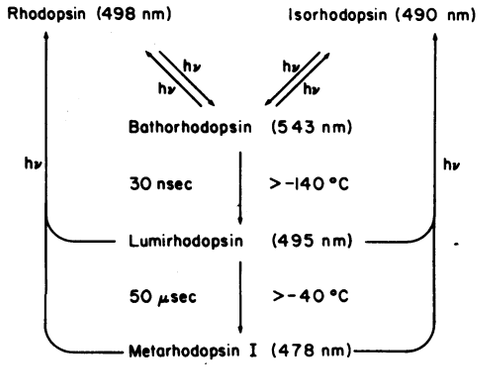

FIG. 2. Partial bleaching sequence of rhodopsin (11-*cis* retinal + opsin) and isorhodopsin (9-*cis* retinal + opsin).

The photostationary steady-state concentrations of bathorhodopsin, rhodopsin, and isorhodopsin under the Raman conditions were determined by the method of Oseroff and Callender (5), except that glycerol glasses were used and the percentages of rhodopsin and isorhodopsin were calculated by a least-squares procedure.

Low temperature spectra were obtained with a standard photon-counting Raman system (13). The monochromator was calibrated on the Rayleigh line and slit widths were 6 cm^{-1}; wavenumber assignments are accurate to ±2 cm^{-1}. Data from identical runs were averaged and smoothed, and fluorescence backgrounds (7,000–30,000 counts/sec) were subtracted by using a PDP 8/e minicomputer. The laser beam at 585 nm was produced by pumping a Coherent 590 dye laser with the all-lines output of a Spectra Physics 165 argon laser.

Room temperature spectra of the photostationary steady state were generated with a Chromatix CMX-4 flash lamp-pumped dye laser. The sample was prepared by sonicating rod outer segments in 50 mM phosphate buffer, pH 7. After centrifugation at 11,000 × *g* for 10 min, the supernatant (20 μM) was made 30 mM in hydroxylamine and pumped at 0.4 ml/min through a 0.5-mm (inside diameter) capillary. For this series of Raman measurements a mismatched subtractive dispersion double monochromator coupled to a dry ice-cooled, intensified vidicon (PAR 1205A and 1205D) was used. The details of this spectrometer will be described later (R. Mathies and N.-T. Yu, unpublished results). The chief advantages of the optical multichannel analyzer (OMA) detection are the increased sensitivity and the extreme speed with which spectra can be generated.

RESULTS

In Fig. 3 we present Raman spectra of photostationary steady-state mixtures of rhodopsin that have been taken with a 488-nm probe and a 585-nm pump in protonated and deuterated media. The population measurements (Table 1) show that the principal effect of turning on the yellow pump beam is to decrease the relative concentration of bathorhodopsin from 55% to 25%. In both the deuterated and protonated media there was a corresponding drop in the intensity of the C=C stretching band of bathorhodopsin (1536 cm^{-1}) compared with that of the overlapping C=C modes of rhodopsin and isorhodopsin (1551 cm^{-1}). In the protonated media (spectra A and B) the C=NH⊕ vibration was seen at 1655 cm^{-1} and it shifted as expected (5) to 1627 cm^{-1} upon deuteration (spectra C and D). The fact that the 1655- and 1627-cm^{-1} bands did not appear to change intensity when the pump beam was used to convert bathorhodopsin back to rhodopsin and isorhodopsin is consistent with the idea that bathorhodopsin has significant scattering at 1655 (1627) cm^{-1}. However, even with very good data this conclusion is not valid unless the contributions of rhodopsin and isorhodopsin to the scattering at 1655 cm^{-1} can be *unambiguously* eliminated.

The spectra in Fig. 4 are analagous to those in Fig. 3 with the roles of the pump and probe reversed. With the yellow 585-nm beam as the probe, the contribution of bathorhodopsin to the Raman spectra will be much more strongly enhanced than either rhodopsin or isorhodopsin. In this way a Raman spectrum of nearly pure bathorhodopsin should be obtained. In Fig. 4 spectra were taken in the presence (A) and absence (B) of a 488-nm pump beam in a protonated medium. The Raman spectrum taken with the probe showed only one major pigment band around 1553 cm^{-1}, the C=C stretch of isorhodopsin. However, when the coaxial blue pump beam was turned on, with pump/probe power ratio at 0.6 to 1, the percent composition of bathorhodopsin rose from 0% to 34% (Table 1), and the yellow probe produced spectacular resonance enhancement

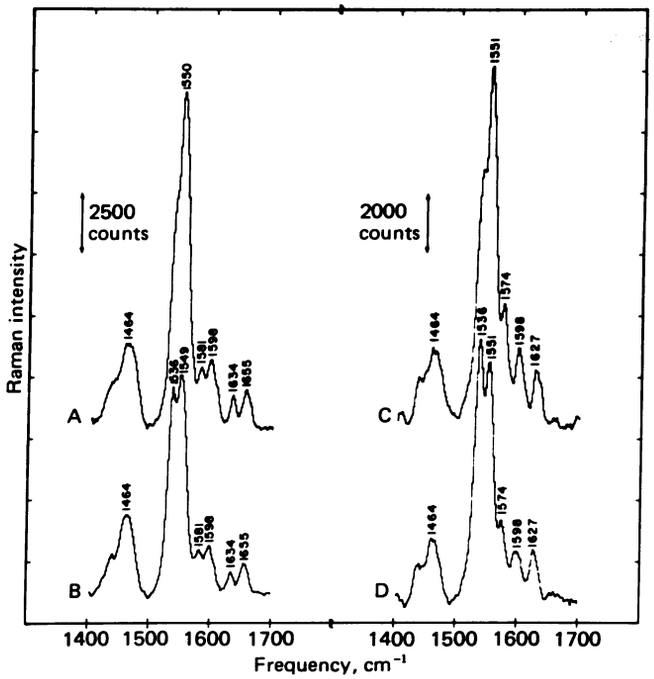

FIG. 3. A and B are resonance Raman spectra of a photostationary steady-state mixture of rhodopsin, isorhodopsin, and bathorhodopsin at −160°C. Spectra were taken with a 488-nm probe beam in the presence (spectrum A) and in the absence (spectrum B) of a coaxial 585-nm pump beam. The pump/probe power ratio is 2.7 to 1. Scattering at 1464 cm^{-1} is due to glycerol. C and D are analogous spectra taken in a deuterated medium.

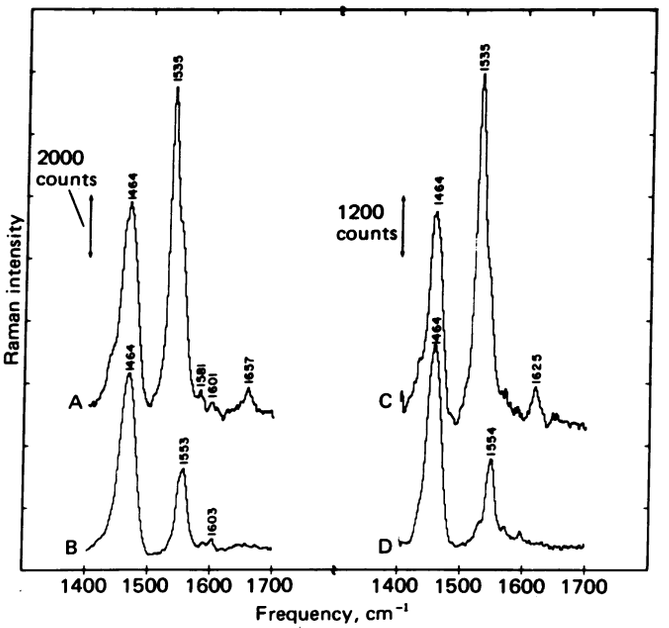

FIG. 4. A and B are resonance Raman spectra of the photostationary steady-state at −160°C. Spectra were taken with a 585-nm probe beam in the presence (spectrum A) and in the absence (spectrum B) of a 488-nm pump beam. The pump/probe power ratio is 0.6 to 1. C and D are analogous spectra in a deuterated medium.

of the 1535-cm^{-1} C=C stretching band of bathorhodopsin. Another resonantly enhanced (bathorhodopsin) line appeared at 1657 cm^{-1} in spectrum A when the blue pump was turned on. This line can be assigned as a C=$NH^{\oplus}$ vibration by the observation that in the deuterated spectra (C and D) this line shifted to 1625 cm^{-1}. This shift is exactly the behavior found in Fig. 3 for mixtures of rhodopsin and isorhodopsin.

Fig. 5 presents the Raman spectrum from 800 to 1700 cm^{-1} of a frozen solution of protonated rhodopsin in Ammonyx LO using a 585-nm probe with (spectrum A) and without (spectrum B) an all-lines blue pump beam. Spectrum A is predominantly bathorhodopsin with some rhodopsin and isorhodopsin. In order to get an essentially pure spectrum of bathorhodopsin, we determined the contributions of isorhodopsin and rhodopsin to spectrum A from the populations in Table 1. The amounts of the isorhodopsin and rhodopsin spectra that must be subtracted are given in spectra B and C, respectively (see below). The final spectrum of bathorhodopsin is given by D. In addition to the expected lines at 853, 875, 920, and 1536 cm^{-1}, lines that can be attributed to bathorhodopsin were found at 1006, 1166, 1210, 1278, 1323, 1437, and 1656 cm^{-1}. The only lines whose intensities were sensitive to the subtraction parameters are those at 966, 1224, and 1240 cm^{-1}. The intensity of the important protonated Schiff base line of bathorhodopsin near 1657 cm^{-1} in spectrum A (Fig. 4) and spectrum D (Fig. 5) was not significantly altered even by obvious oversubtractions of rhodopsin and isorhodopsin.

Table 1. Photostationary steady-state compositions at −160°C

Probe, nm	Pump, nm	Pump/probe power ratio	Batho-rhodopsin	Rho-dopsin	Isorho-dopsin
488			55	32	13
488	585	2.7	25	48	27
585	488	0.63	34	43	23
585	All-lines	3.5	45	39	16
585			0	<5	>95

Compositions are accurate to ±5%.

The amounts of isorhodopsin and rhodopsin that must be subtracted in Fig. 5 were determined in the following manner. The fraction of the 585-nm probe spectrum (isorhodopsin) was determined by scaling the probe-only spectrum by the percentage of isorhodopsin (16%) in the all-lines pump plus probe experiment (see Table 1). A room temperature Raman spectrum of pure rhodopsin probed at 600 nm was obtained from ref. 13. It was scaled to the Raman spectrum of isorhodopsin through the relative Raman scattering cross sections for the ethylenic lines of rhodopsin and isorhodopsin at 585 nm ($\sigma_R/\sigma_I = 1.5 \pm 0.1$). These relative Raman cross sections were determined from rapid flow experiments on purified rhodopsin and isorhodopsin (13) by measurement of the relative intensities of the ethylenic line for each molecule. The resulting rhodopsin spectrum was then scaled by the percentage of rhodopsin in the pump plus probe experiment (39%). The use of a rhodopsin spectrum obtained at room temperature rather than at −160°C is qualitatively justified by the observation that room temperature (13) and low temperature (5) spectra of isorhodopsin are virtually identical.

Fig. 6 displays the Raman spectrum at room temperature of sonicated rod outer segment membranes with 1-μsec, 2-kW pulses from a dye laser at 488 nm with OMA detection. When the laser intensity is sufficiently high, a photostationary steady state containing rhodopsin, isorhodopsin, and bathorhodopsin will be generated. This approach has already been used to produce a photostationary steady state between the BR_{570} and K species in the purple membrane from *Halobacterium halobium* (19). By using the best available estimates of the appropriate rate constants, extinction coefficients, and quantum yields, we calculate that our room temperature pulsed spectra should have the same relative composition as those generated

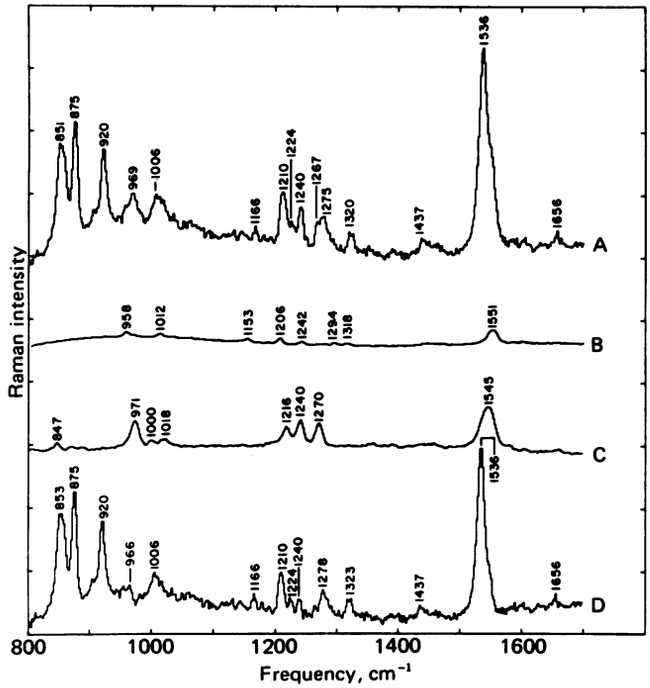

FIG. 5. A and B are resonance Raman spectra of the photostationary steady-state at −160°C. Spectra (in Ammonyx LO) were taken with a 585-nm probe beam in the presence (Spectrum A) and in the absence (spectrum B) of an all-lines argon ion pump beam. The pump/probe power ratio is 3.5. C is the rapid-flow resonance Raman spectrum of rhodopsin taken with a 600-nm probe beam (from ref. 13). D is the resonance Raman spectrum of pure bathorhodopsin obtained by subtracting the appropriate amounts (see text) of isorhodopsin (spectrum B) and rhodopsin (spectrum C) from spectrum A.

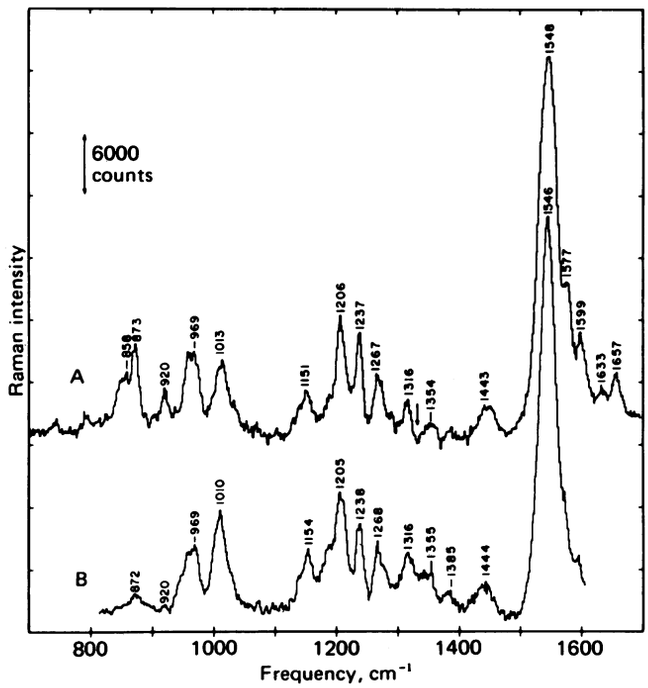

FIG. 6. Resonance Raman spectra of sonicated rod outer segment membranes at room temperature taken with an OMA detection system. Spectrum A was taken with 488-nm, 2-kW peak power pulses (50-mW average power at 20 Hz) which were focused on the sample with a 50-mm lens. The spectrum is composed of two overlapping OMA scans that have been joined at about 1325 cm^{-1} (arrow). The slit width was 100 μm (7.3 cm^{-1}). Spectrum B was taken under identical conditions with a 50-mW continuous wave (CW) 488-nm beam.

at low temperature with 488-nm irradiation. Spectrum A clearly shows the presence of characteristic bathorhodopsin lines at 858, 873, and 920 cm^{-1} as well as a slight broadening of the ethylenic line on the low cm^{-1} side. These features are not observed in spectrum B obtained under the same conditions with a 50-mW CW 488-nm probe beam. Even though bathorhodopsin decays to lumirhodopsin with a lifetime of 30 nsec (Fig. 2), no large steady state concentration of lumi will be maintained in the laser beam. This is because the *light-dependent* rate constants for converting lumirhodopsin back to its parent pigments rhodopsin and isorhodopsin ($\approx 10^9$ sec^{-1}) are much larger than the *light-independent* rate constants for the decay of bathorhodopsin to lumirhodopsin (3×10^7 sec^{-1}) (4). In the CW experiment this is not true because the light-dependent rate constant for reconversion of lumirhodopsin is much smaller ($\approx 10^4$ sec^{-1}).

DISCUSSION

The principal conclusion from this work is that the chromophore of bathorhodopsin is linked to opsin through a protonated Schiff base. In Fig. 4 the near coincidence of the stretching frequency of the Schiff base bond of bathorhodopsin (1657 cm^{-1}) with that of isorhodopsin (1654–1655 cm^{-1}) (5, 13) and rhodopsin (1657–1660 cm^{-1}) (13, 14) shows that *no net change in the C=NH⊕ bond order occurs upon going from rhodopsin or isorhodopsin to bathorhodopsin*. Furthermore, the fact that the C=NH⊕ bond of bathorhodopsin has nearly the same shift upon deuteration (1657 → 1625 cm^{-1}) as does rhodopsin and isorhodopsin (1655 → 1627 cm^{-1}) indicates that the contribution of the hydrogen (deuterium) to the reduced mass of the Schiff base vibration is not significantly altered by the conversion to bathorhodopsin. *Hence the N—H bond strength does not change when bathorhodopsin is produced.* These conclusions provide critical evidence that can be used to evaluate proposed models for the structure of retinal in bathorhodopsin.

Fig. 1 presents three examples of valence bond structures that have been proposed by Fransen *et al.* (6), van der Meer *et al.* (7), and Peters *et al.* (8) as models for bathorhodopsin. All of them assume that a proton transfer from opsin to retinal constitutes the initial photochemical event. To the extent that these simple valence bond structures apply, they predict that the Schiff base C=NH⊕ bond order should be dramatically reduced and the N—H bond order increased in the conversion to bathorhodopsin. These predictions are clearly inconsistent with our Raman results. However, our data do not explicitly exclude the possibility of proton translocation in the formation of bathorhodopsin. They simply require that, by the time ground-state bathorhodopsin is formed, the C=NH⊕ and N—H bonds be restored to their original strengths. One possible mechanism involving the Schiff base proton begins with excitation of rhodopsin to a high vibrational level of its excited electronic state. Vibrational and conformational relaxation proceeds in the excited state with a transfer of the Schiff base proton toward the nitrogen; after radiationless decay to an excited vibrational level of the ground electronic state, relaxation again occurs with *reverse* proton transfer to give ground state bathorhodopsin. Similar models have been proposed to describe the double proton transfer in 7-azaindole dimers (20) and intramolecular proton transfer in azole derivatives (21). A second possibility is that the proton transfer could be caused elsewhere in the protein by the light-induced charge shift in electronically excited retinal (22, 23). Such a qualitative model has been proposed by Lewis (24). Also, Warshel (25) has provided quantitative calculations justifying simultaneous contributions

from both retinal and opsin reaction coordinates. Another possibility is that the initial event is simply a photoisomerization to a distorted but nearly all-*trans* conformation of the retinal chromophore (26). This could of course occur in conjunction with any of the proton transfer mechanisms considered above and need not be considered exclusively.

The idea that a retroretinal or analogous structure (Fig. 1) can be formed while the C=NH⊕ total bond strength is unchanged has been considered by several authors (refs. 7, 24, 25; A. Warshel, personal communication). If this is true, then our data on the Schiff base linkage alone cannot be used to criticize these models. However, no *quantitative* prediction of the changes in the carbon-nitrogen bond strength in these circumstances has been given. Our data show that the Schiff base vibrational frequency in bathorhodopsin differs from that of rhodopsin (isorhodopsin) by less than 0.5%. Credibility of such models will attend the theoretical description of a retrostructure which preserves the C=N frequency to this accuracy.

The fingerprint regions of visual pigment Raman spectra (1100–1400 cm^{-1}) have been shown to be similar to those of the corresponding protonated *n*-butylamine Schiff base retinals (12). However, the fingerprint region of bathorhodopsin (Fig. 5, spectrum D) does not bear a strong resemblance to either the 11-*cis* or all-*trans* protonated Schiff base derivatives of retinal (12). Moreover, the three characteristic lines of bathorhodopsin at 853, 875, and 920 cm^{-1} are not found in the model compounds. Fransen *et al.* (6) have attempted to explain these lines in terms of a retrotautomer of the 11-*cis* chromophore containing an exomethylene double bond (Fig. 1). However, this model would seem to require a reduction of the C=NH⊕ bond order in bathorhodopsin, and we have shown that this does not occur. It should be noted that Warshel (27) has calculated that torsional modes of the β-ionyl ring could also account for these unique lines. A more positive statement about the conformation of the chromophore in bathorhodopsin should be possible when experiments of the type described here are performed on visual pigment analogues.

In our pulsed laser experiments, we have succeeded in generating a photostationary steady-state mixture of rhodopsin, isorhodopsin, and bathorhodopsin at room temperature by using high light intensities ($\approx 5 \times 10^{25}$ photon/cm^2 per sec at 488 nm). During the laser pulse we observe scattering at 858, 873, and 920 cm^{-1} that is characteristic of the unique, intense bathorhodopsin lines which have been previously observed only at low temperature. This indicates that these low wavenumber lines of bathorhodopsin are not the result of a strained chromophore conformation that is trapped at low temperature by the frozen protein matrix. Therefore, the spectrum of pure bathorhodopsin that we generated from the low temperature data should provide a relevant description of the conformation of retinal in bathorhodopsin when this spectrum is theoretically analyzed. The mean lifetime of a particular species in this photostationary steady state can be calculated by using the light intensity as well as the appropriate extinction coefficients and quantum yields for the various constituents. Under the conditions of our experiment, the mean lifetime of bathorhodopsin was 1 nsec. Thus the scattering observed from bathorhodopsin comes on the average from molecules that have been allowed to conformationally relax for about 1 nsec. The "time scale" of the pulsed experiment is *not* dictated by the pulse duration but by the light intensity, because the light-dependent rates are so much larger than the light-independent rates. Doukas *et al.* (16) have shown that metarhodopsin I does not exhibit these low wavenumber lines and looks like an all-*trans* chromophore. Therefore, Raman measurements of the conversion of bathorhodopsin → lumirhodopsin and lumirhodopsin → metarhodopsin I should provide evidence concerning the origin of these unique bathorhodopsin lines.

We thank Profs. Wayne Hubbell and I. Tinoco, Jr. for the use of their dark room and minicomputer facilities, respectively. We are indebted to Bostick Curry for writing the Raman data analysis programs. This work was supported by grants from the National Eye Institute (EY-02051), the American Chemical Society Petroleum Research Fund (9774-G1,6), Research Corporation, the Berkeley Biomedical Research Support Grant (RR 07006), and the Committee on Research, University of California, Berkeley. G.E. is a National Science Foundation Predoctoral Fellow.

1. Wald, G. (1968) *Nature (London)* **219**, 800–807.
2. Hubbard, R. & Kropf, A. (1958) *Proc. Natl. Acad. Sci. USA* **44**, 130–139.
3. Yoshizawa, T. & Wald, G. (1963) *Nature (London)* **197**, 1279–1286.
4. Busch, G. E., Applebury, M. L., Lamola, A. A. & Rentzepis, P. M. (1972) *Proc. Natl. Acad. Sci. USA* **69**, 2802–2806.
5. Oseroff, A. R. & Callender, R. H. (1974) *Biochemistry* **13**, 4243–4248.
6. Fransen, M. R., Luyten, W. C. M. M., van Thuijl, J., Lugtenburg, J., Jansen, P. A. A., van Breugel, P. J. G. M. & Daemen, F. J. M. (1976) *Nature (London)* **260**, 726–727.
7. van der Meer, K., Mulder, J. J. C. & Lugtenburg, J. (1976) *Photochem. Photobiol.* **24**, 363–367.
8. Peters, K., Applebury, M. L. & Rentzepis, P. M. (1977) *Proc. Natl. Acad. Sci. USA* **74**, 3119–3123.
9. Kropf, A. (1976) *Nature (London)* **264**, 92–94.
10. Green, B. H., Monger, T. G., Alfano, R. R., Aton, B. & Callender, R. H. (1977) *Nature (London)* **269**, 179–180.
11. Hurley, J. B., Ebrey, T. G., Honig, B. & Ottolenghi, M. (1977) *Nature (London)* **270**, 540–542.
12. Mathies, R., Freedman, T. B. & Stryer, L. (1977) *J. Mol. Biol.* **109**, 367–372.
13. Mathies, R., Oseroff, A. R. & Stryer, L. (1976) *Proc. Natl. Acad. Sci. USA* **73**, 1–5.
14. Callender, R. H., Doukas, A., Crouch, R. & Nakanishi, K. (1976) *Biochemistry* **15**, 1621–1629.
15. Sulkes, M., Lewis, A., Lemley, A. T. & Cookingham, R. (1976) *Proc. Natl. Acad. Sci. USA* **73**, 4266–4270.
16. Doukas, A. G., Aton, B., Callender, R. H. & Ebrey, T. G. (1978) *Biochemistry* **17**, 2430–2435.
17. Hong, K. & Hubbell, W. L. (1973) *Biochemistry* **12**, 4517–4523.
18. Applebury, M. L., Zuckerman, D. M., Lamola, A. A. & Jovin, T. M. (1974) *Biochemistry* **13**, 3448–3458.
19. Goldschmidt, C. R., Ottolenghi, M. & Korenstein, R. (1976) *Biophys. J.* **16**, 839–843.
20. Ingham, K. C. & El-Bayoumi, M. A. (1974) *J. Am. Chem. Soc.* **96**, 1674–1682.
21. Williams, D. L. & Heller, A. (1970) *J. Phys. Chem.* **74**, 4473–4480.
22. Salem, L. & Bruckmann, P. (1975) *Nature (London)* **258**, 526–528.
23. Mathies, R. & Stryer, L. (1976) *Proc. Natl. Acad. Sci. USA* **73**, 2169–2173.
24. Lewis, A. (1978) *Proc. Natl. Acad. Sci. USA* **75**, 549–553.
25. Warshel, A. (1978) *Proc. Natl. Acad. Sci. USA* **75**, 2558–2562.
26. Rosenfeld, T., Honig, B., Ottolenghi, M., Hurley, J. & Ebrey, T. G. (1977) *Pure Appl. Chem.* **49**, 341–351.
27. Warshel, A. (1977) *Annu. Rev. Biophys. Bioeng.* **6**, 273–300.